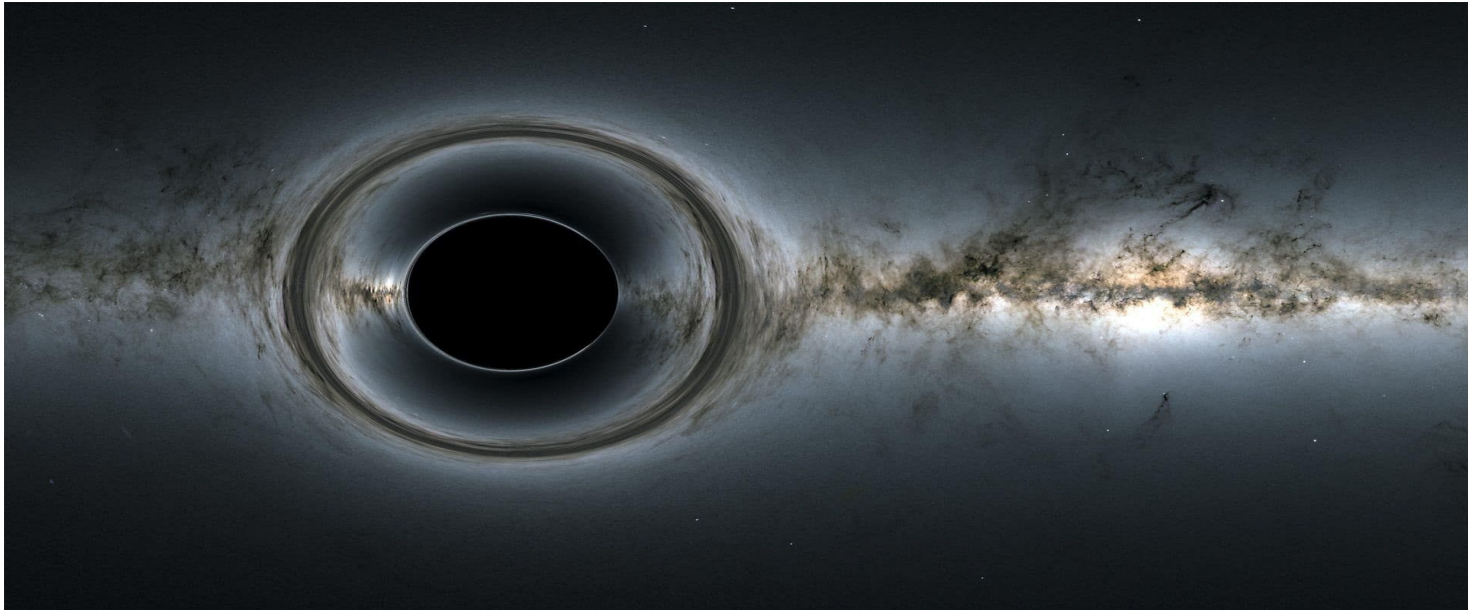# Constraining Electromagnetic Signals from Black Holes with Hair

Nicole Crumpler
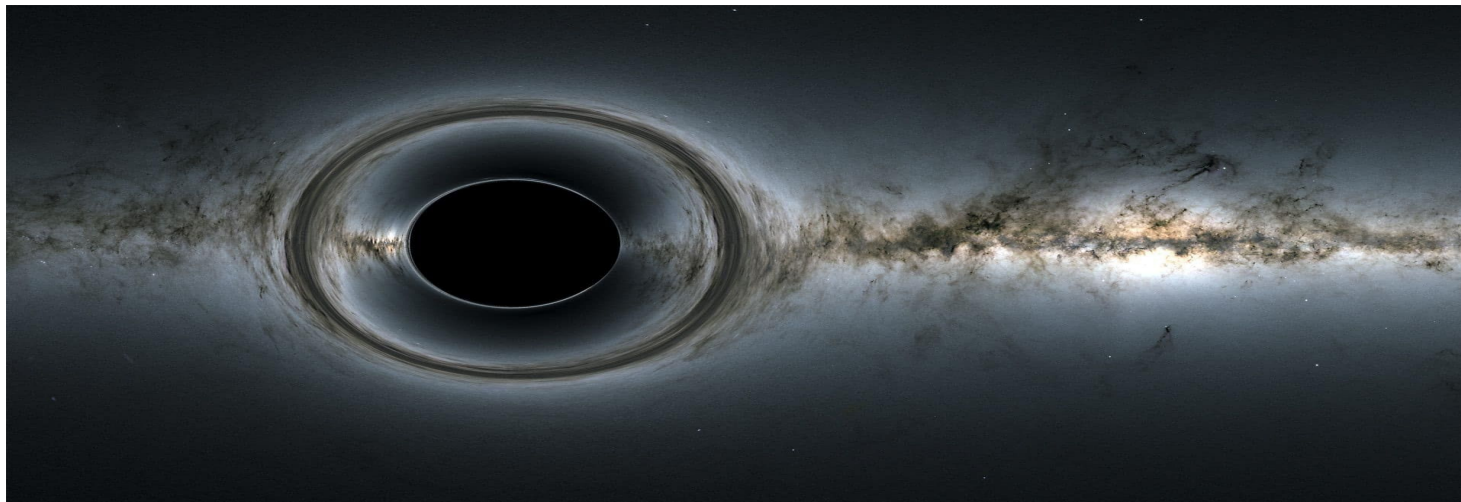### Collaborators: David Kaplan, Surjeet Rajendran

Motivation

- "No Hair" Theorem for Black Holes (BHs)
    - Stationary BHs fully characterized by mass, charge, and spin

Motivation

- "No Hair" Theorem for Black Holes (BHs)
    - Stationary BHs fully characterized by mass, charge, and spin
- Leads to BH Information Paradox
    - Possibility of richer physics, BHs with "hair" leading to unique observable signatures
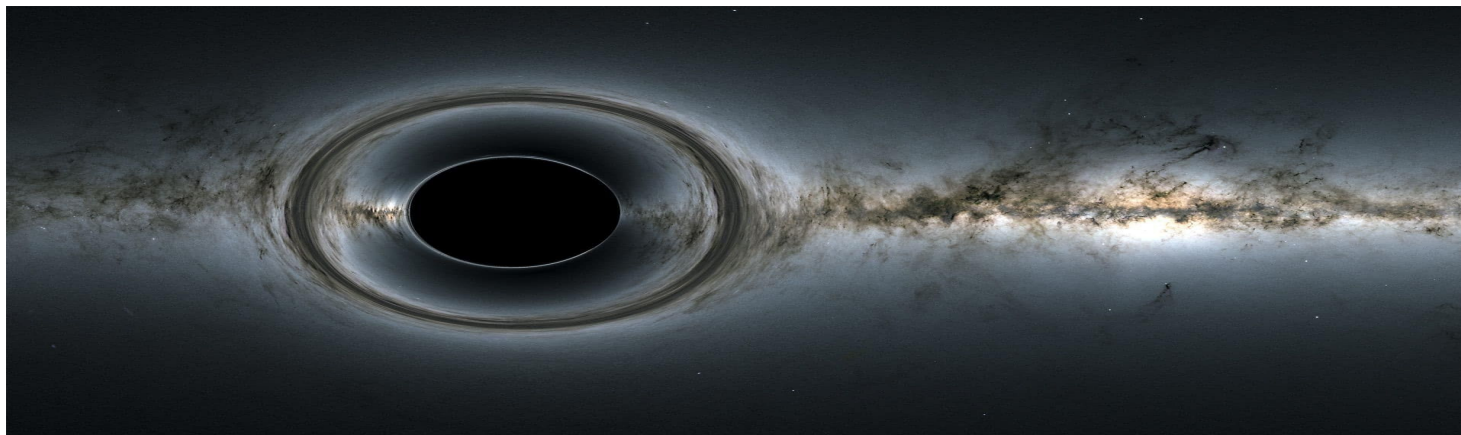

Nicole Crumpler

Motivation

- "No Hair" Theorem for Black Holes (BHs)
  - Stationary BHs fully characterized by mass, charge, and spin
- Leads to BH Information Paradox
  - Possibility of richer physics, BHs with "hair" leading to unique observable signatures
- Electromagnetic (EM) radiation is one of simplest signatures to observe

Motivation

- "No Hair" Theorem for Black Holes (BHs)
  - Stationary BHs fully characterized by mass, charge, and spin
- Leads to BH Information Paradox
  - Possibility of richer physics, BHs with "hair" leading to unique observable signatures
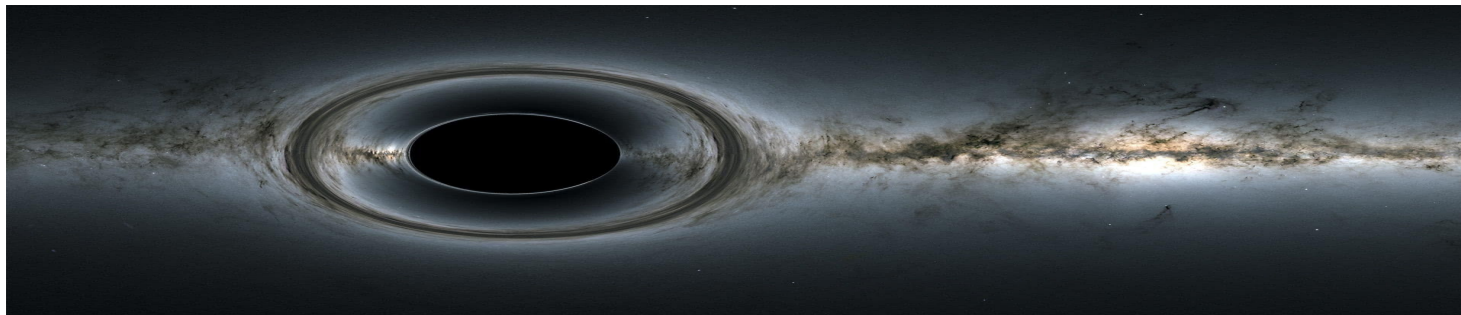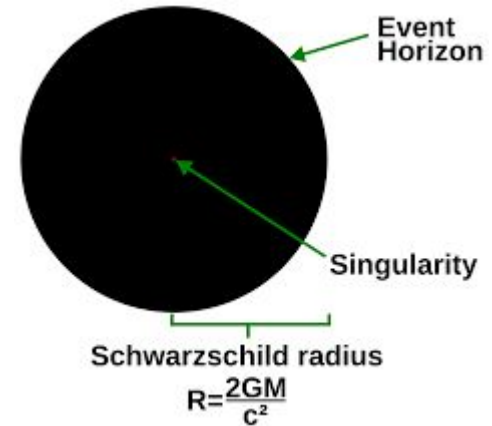- Electromagnetic (EM) radiation is one of simplest signatures to observe
- Investigate observational signatures of BH releasing some of its mass as EM radiation

Preliminaries

- Any radiation emitted by the BH must tunnel out of gravitational well in same manner as Hawking radiation
    - Frequency $f = 1/2r_s$ depends ONLY on BH mass (very model independent!)

Event Horizon

Singularity

Schwarzschild radius
$R = \frac{2GM}{c^2}$

Preliminaries

- Any radiation emitted by the BH must tunnel out of gravitational well in same manner as Hawking radiation
  - Frequency $f = 1/2r_s$ depends ONLY on BH mass (very model independent!)
- Proportion of BH mass released as EM radiation characterized by dimensionless ϵ
  - $E_{BH} = \epsilon M_{BH}$

Event Horizon

Singularity
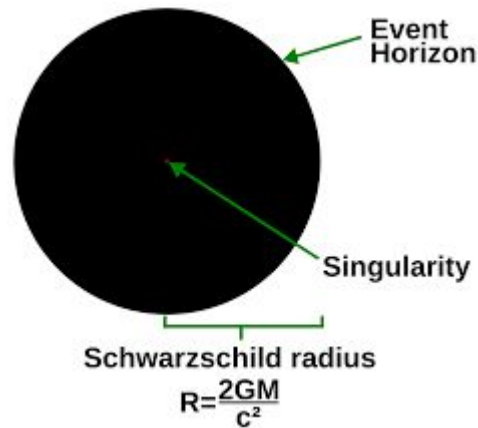
Schwarzschild radius
$R = \frac{2GM}{c^2}$

Preliminaries

- Any radiation emitted by the BH must tunnel out of gravitational well in same manner as Hawking radiation
  - Frequency $f = 1/2r_s$ depends ONLY on BH mass (very model independent!)
- Proportion of BH mass released as EM radiation characterized by dimensionless ϵ
  - $E_{BH} = \epsilon M_{BH}$
- Low frequency radio waves, absorbed by interstellar medium
  - Not directly observable, must be absorbed and re-emitted

Preliminaries

- Any radiation emitted by the BH must tunnel out of gravitational well in same manner as Hawking radiation
    - Frequency f = 1/2r_s depends ONLY on BH mass (very model independent!)
- Proportion of BH mass released as EM radiation characterized by dimensionless ϵ
    - $E_{BH}=\epsilon M_{BH}$
- Low frequency radio waves, absorbed by interstellar medium
    - Not directly observable, must be absorbed and re-emitted
- BH-BH merger as trigger for the event
    - Must be observable extragalactically (> 100 Mpc), so very energetic (large ϵ)

Goal

- **Constrain broad class of "hairy" BH models using a generic and model-independent EM signal that is fully characterized by the BH mass (M) and the proportion of that mass that is lost to EM radiation (ϵ)**

Goal

- **Constrain broad class of "hairy" BH models using a generic and model-independent EM signal that is fully characterized by the BH mass (M) and the proportion of that mass that is lost to EM radiation (ϵ)**
- Place an upper bound on ϵ using existing telescope observations and to motivate X-ray and gamma-ray observations of BH-BH mergers
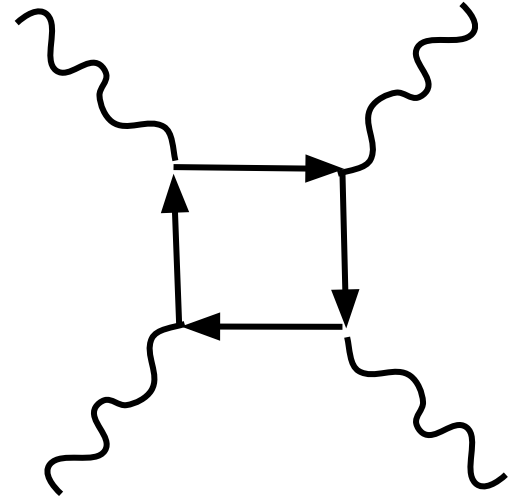
Chandra X-ray Observatory

Fermi Gamma-ray Space Telescope
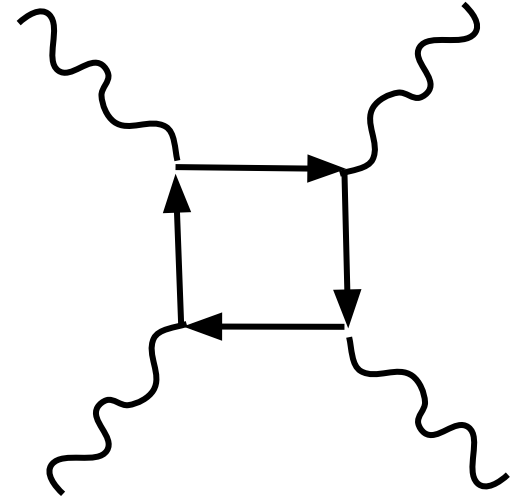
Nicole Crumpler

Schwinger Limit

- Nature of re-emitted radiation depends on if field strength surpasses this limit

Schwinger Limit

- Nature of re-emitted radiation depends on if field strength surpasses this limit
- Schwinger Limit: Point at which the EM field energy density is great enough for spontaneous electron-positron pair production
  - $E_C = m_e^2/e = 0.86$ MeV^2
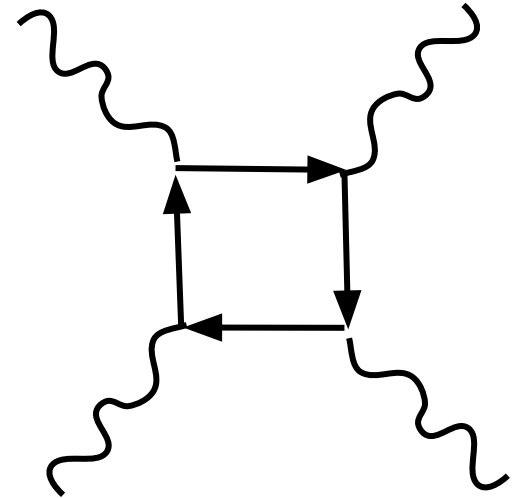
Schwinger Limit

- Nature of re-emitted radiation depends on if field strength surpasses this limit
- Schwinger Limit: Point at which the EM field energy density is great enough for spontaneous electron-positron pair production
  - $E_C = m_e^2/e = 0.86$ MeV^2
- The critical value of ϵ is $\epsilon_C \sim 2.6 \times 10^{-10} M^2$ where M is the BH mass in solar units

Gamma-ray Emission Above the Schwinger Limit

- For $\epsilon > \epsilon_C$, pair-production results in electron-positron fireball
  - Classic production mechanism for GRB

Gamma-ray Emission Above the Schwinger Limit

- For $\epsilon > \epsilon_C$, pair-production results in electron-positron fireball
  - Classic production mechanism for GRB
- Fireball thermalizes due to Thompson scattering and expands relativistically as an ideal fluid

Gamma-ray Emission Above the Schwinger Limit

- For $\epsilon > \epsilon_C$, pair-production results in electron-positron fireball
  - Classic production mechanism for GRB
- Fireball thermalizes due to Thompson scattering and expands relativistically as an ideal fluid
- Initial temperature, $T_0 = (E/V_0 g_0 a)^{¼} \sim 200(\epsilon/M^2)^{1/4}$ MeV

Gamma-ray Emission Above the Schwinger Limit

- For $\epsilon > \epsilon_C$, pair-production results in electron-positron fireball
  - Classic production mechanism for GRB
- Fireball thermalizes due to Thompson scattering and expands relativistically as an ideal fluid
- Initial temperature, $T_0 = (E/V_0 g_0 a)^{\frac{1}{4}} \sim 200(\epsilon/M^2)^{1/4}$ MeV
- Temperature in lab frame is constant, $T(r) = T_0$
  - Adiabatic expansion into vacuum

Gamma-ray Emission Above the Schwinger Limit

- For $\epsilon > \epsilon_C$, pair-production results in electron-positron fireball
  - Classic production mechanism for GRB
- Fireball thermalizes due to Thompson scattering and expands relativistically as an ideal fluid
- Initial temperature, $T_0 = (E/ V_0 g_0 a)^{1/4} \sim 200(\epsilon/M^2)^{1/4}$ MeV
- Temperature in lab frame is constant, $T(r) = T_0$
  - Adiabatic expansion into vacuum
- Temperature in comoving frame decreases, $T'(r) \propto T_0/r$ until pair-production freezes out

Gamma-ray Emission Above the Schwinger Limit

- Photons free stream as black body radiation

Figure 1. This plot shows the peak photon energy as a function of BH mass and ϵ. These peak energies are > 1 MeV and so are gamma rays.

Gamma-ray Emission Above the Schwinger Limit

- Photons free stream as black body radiation
- O(1) of energy released by BH is emitted in photons at peak energy of spectrum
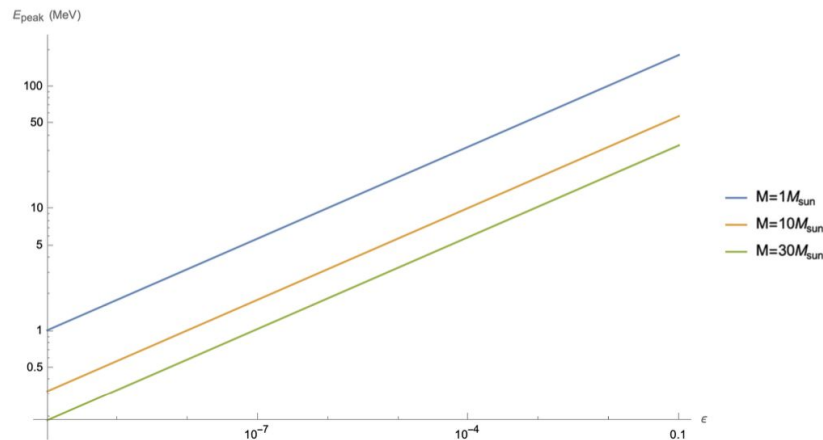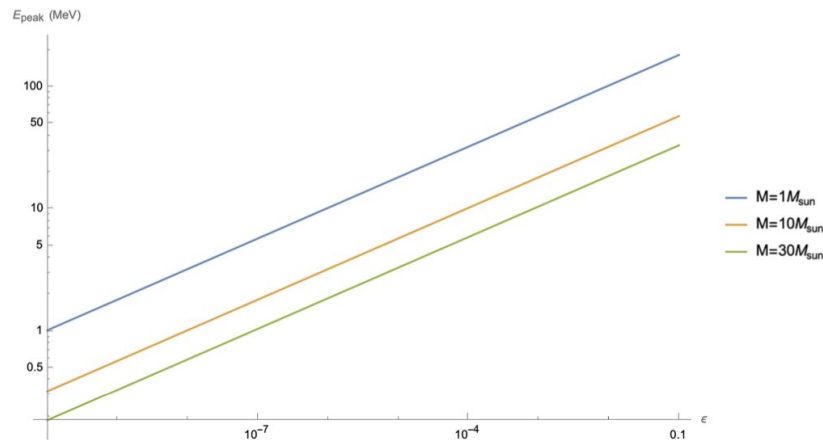

Figure 1. This plot shows the peak photon energy as a function of BH mass and ϵ. These peak energies are > 1 MeV and so are gamma rays.

Gamma-ray Emission Above the Schwinger Limit

- Fermi-GBM is most sensitive telescope
    - Sensitivity limits require flux of ~1 ph cm^{-2}
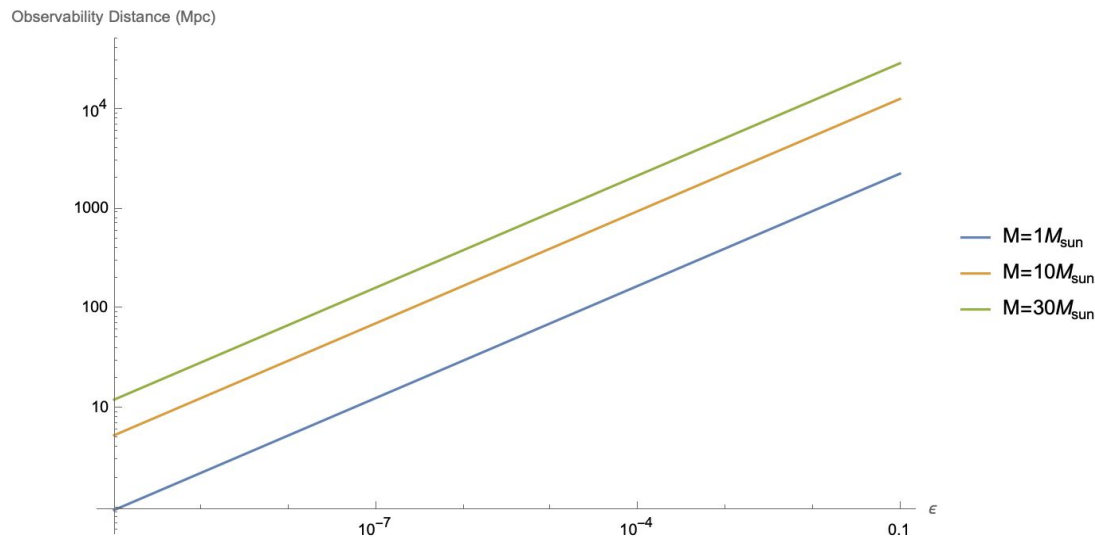
Gamma-ray Emission Above the Schwinger Limit

- Fermi-GBM is most sensitive telescope
    - Sensitivity limits require flux of ~1 ph cm^{-2}
- Observability distance d~5362 $\epsilon^{3/8}$M$^{3/4}$ Mpc

Gamma-ray Emission Above the Schwinger Limit

- Fermi-GBM is most sensitive telescope
  - Sensitivity limits require flux of ~1 ph cm^{-2}
- Observability distance d~5362 $\epsilon^{3/8}$M$^{3/4}$ Mpc
- Many BH-BH mergers observed by LIGO/Virgo were also observed by Fermi-GBM

Gamma-ray Emission Above the Schwinger Limit

- Fermi-GBM is most sensitive telescope
  - Sensitivity limits require flux of ~1 ph cm^{-2}
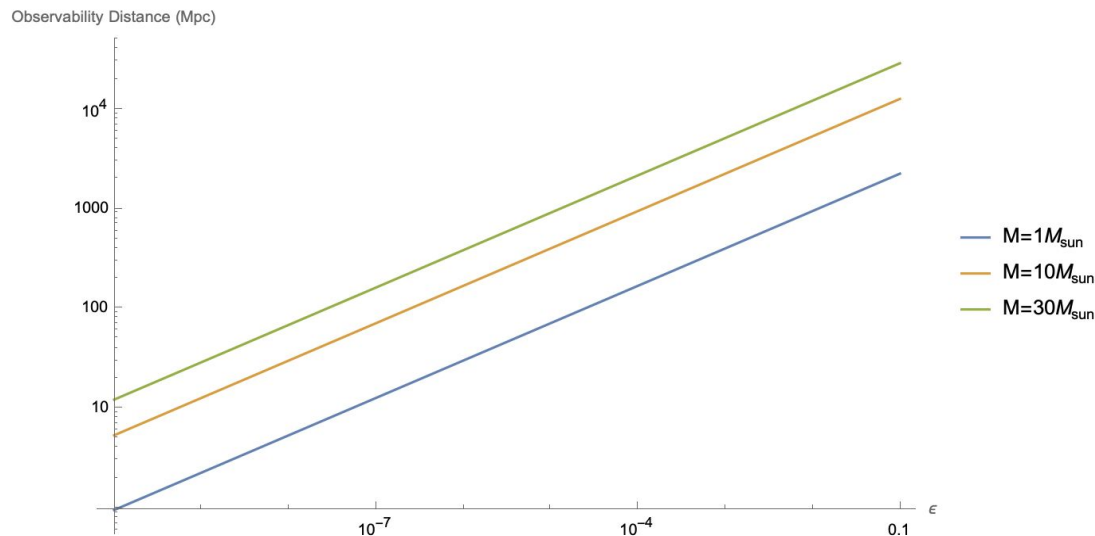- Observability distance d~5362 $\epsilon^{3/8}$M$^{3/4}$ Mpc
- Many BH-BH mergers observed by LIGO/Virgo were also observed by Fermi-GBM
- Non-detection of GRB from BH-BH mergers for which Fermi-GBM was observing >90% of GW localization region can be used to constrain ϵ
  - Assuming all BHs are "hairy" BHs capable of this emission

Gamma-ray Emission Above the Schwinger Limit

Id	$O(m)/M_\odot$	$m_1/M_\odot$	$m_2/M_\odot$	d_L/Mpc	% LR Observed	ϵ_{Min}	E_{Peak}/MeV
GW191216_213338-v1	10	$12.1^{+4.6}_{-2.3}$	$7.7^{+1.6}_{-1.9}$	340^{+120}_{-130}	99.8	1.4×10^{-5}	6.3
GW190915_235702-v2	20	$32.6^{+8.8}_{-4.9}$	$24.5^{+4.9}_{-5.8}$	1750^{+710}_{-650}	98.0	3.1×10^{-4}	9.6
GW190412_053044-v4	30	$27.7^{+6.0}_{-6.0}$	$9^{+2.0}_{-1.4}$	720^{+240}_{-220}	99.8	1.1×10^{-5}	3.4
GW190521_074359-v2	40	$43.4^{+5.8}_{-5.5}$	$33.4^{+5.2}_{-6.8}$	1080^{+580}_{-530}	100.0	2.7×10^{-5}	3.7
GW190701_203306-v2	50	$54.1^{+12.6}_{-8.0}$	$40.5^{8.7}_{-12.1}$	2090^{+770}_{-740}	100.0	7.5×10^{-5}	4.3

Table 1. For each event used to constrain a particular mass range, this table lists the GWTC Id, the constrained mass order of magnitude($O(m)$), the measured constituent BH masses (m_1, m_2), the measured luminosity distance (d_L), the percent of the LR observed by the Fermi-GBM, the constraint on ϵ from the non-detection of a corresponding GRB by Fermi, and the peak photon energy of a GRB corresponding to ϵ_{min}.

Gamma-ray Emission Above the Schwinger Limit

- 1s short GRB observed by Fermi-GBM 0.4s after GW150914
  - Localization consistent with GW signal

Fig. 1.— Localization map for GW150914, the GW event reported in Abbott et al. (2016). The grey shaded region indicates the region of sky occulted to *Fermi* by the Earth at the time of GW150914. The region not occulted by the Earth contains 75% of the probability of the localization map, with all but 6% of the probability contained in the southern portion of the annulus. The entire region was visible to *Fermi* GBM 25 minutes after the GW event was detected.

Figure from Connaughton 2016

Gamma-ray Emission Above the Schwinger Limit

- 1s short GRB observed by Fermi-GBM 0.4s after GW150914
  - Localization consistent with GW signal
- The GRB cannot be confidently associated with the GW signal
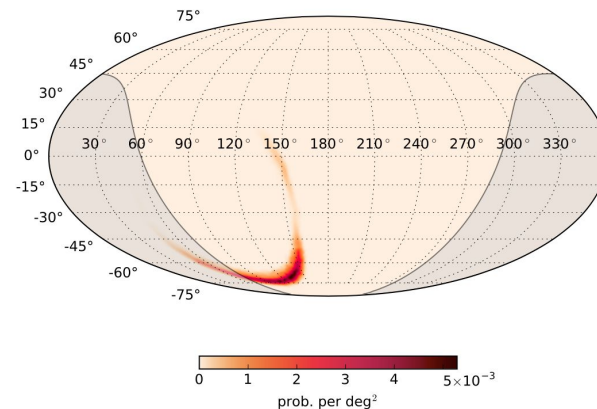 - Near detection threshold (2.9 σ)

Fig. 1.— Localization map for GW150914, the GW event reported in Abbott et al. (2016). The grey shaded region indicates the region of sky occulted to *Fermi* by the Earth at the time of GW150914. The region not occulted by the Earth contains 75% of the probability of the localization map, with all but 6% of the probability contained in the southern portion of the annulus. The entire region was visible to *Fermi* GBM 25 minutes after the GW event was detected.

Figure from Connaughton 2016

Gamma-ray Emission Above the Schwinger Limit

- 1s short GRB observed by Fermi-GBM 0.4s after GW150914
  - Localization consistent with GW signal
- The GRB cannot be confidently associated with the GW signal
  - Near detection threshold (2.9 σ)
- Observed GRB is consistent with rapid EM emission via this mechanism for a 30-40 M⊙ BH and $\epsilon \sim 10^{-7}$-10^{-6}
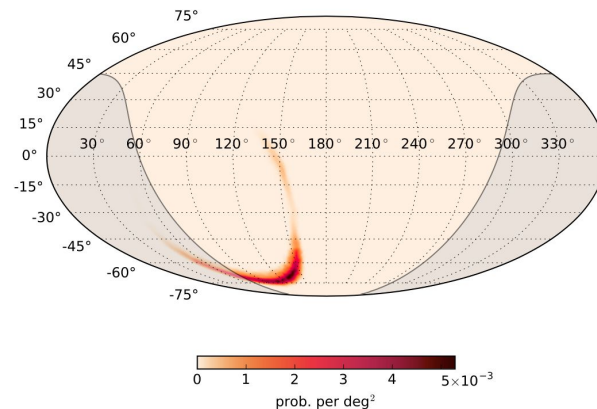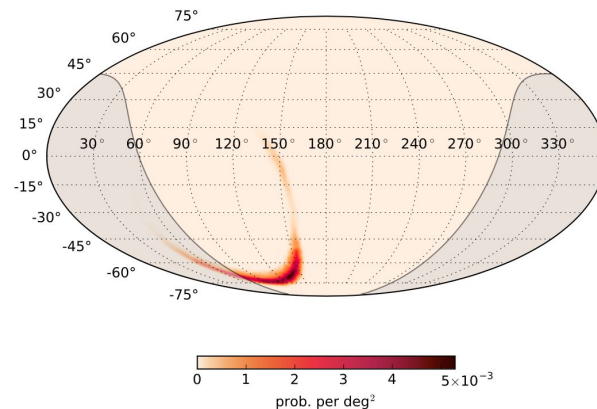

Fig. 1.— Localization map for GW150914, the GW event reported in Abbott et al. (2016). The grey shaded region indicates the region of sky occulted to *Fermi* by the Earth at the time of GW150914. The region not occulted by the Earth contains 75% of the probability of the localization map, with all but 6% of the probability contained in the southern portion of the annulus. The entire region was visible to *Fermi* GBM 25 minutes after the GW event was detected.

Figure from Connaughton 2016

Galactic Cosmic Ray Signal Below the Schwinger Limit

- For $\epsilon < \epsilon_C$, strong EM field accelerates ambient charged particles

Figure 7. This plot shows the fractional energy remaining in the field as a function of distance from the BH for a 1 $M_\odot$ BH and initial energy of $\epsilon M_{BH} = 10^{-10} M_\odot$. For this ϵ, the absorption length is $j_{abs} \sim 6 \times 10^8$ wavelengths.

Galactic Cosmic Ray Signal Below the Schwinger Limit

- For $\epsilon < \epsilon_C$, strong EM field accelerates ambient charged particles
- Solve for particle motion in BH EM field
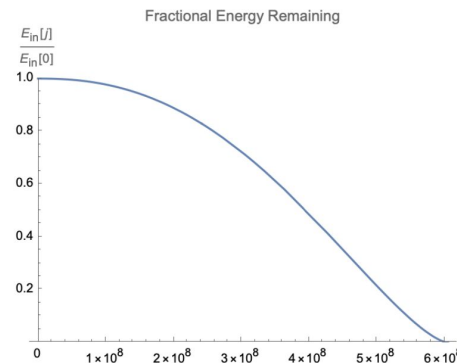
Figure 7. This plot shows the fractional energy remaining in the field as a function of distance from the BH for a 1 $M_\odot$ BH and initial energy of $\epsilon M_{BH} = 10^{-10} M_\odot$. For this ϵ, the absorption length is $j_{abs} \sim 6 \times 10^8$ wavelengths.

Galactic Cosmic Ray Signal Below the Schwinger Limit

- For $\epsilon < \epsilon_C$, strong EM field accelerates ambient charged particles
- Solve for particle motion in BH EM field
- Gives equation for absorption of energy as EM field from BH propagates outwards
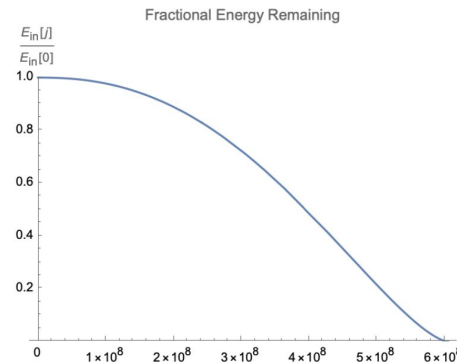 - Characteristic absorption length
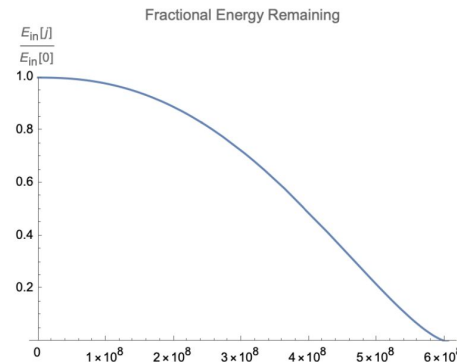
Figure 7. This plot shows the fractional energy remaining in the field as a function of distance from the BH for a 1 $M_\odot$ BH and initial energy of $\epsilon M_{BH} = 10^{-10} M_\odot$. For this ϵ, the absorption length is $j_{abs} \sim 6 \times 10^8$ wavelengths.

Galactic Cosmic Ray Signal Below the Schwinger Limit

- Absorption length fixes average energy per particle, these are Cosmic Ray (CR) energies

Galactic Cosmic Ray Signal Below the Schwinger Limit

- Absorption length fixes average energy per particle, these are Cosmic Ray (CR) energies
- Produce protons with energies ~10 GeV-10 TeV and electrons with energies of ~0.01-10 GeV, how would we observe these particles?

Galactic Cosmic Ray Signal Below the Schwinger Limit

- Absorption length fixes average energy per particle, these are Cosmic Ray (CR) energies
- Produce protons with energies ~10 GeV-10 TeV and electrons with energies of ~0.01-10 GeV, how would we observe these particles?
- Larmor radiation

Galactic Cosmic Ray Signal Below the Schwinger Limit

- Absorption length fixes average energy per particle, these are Cosmic Ray (CR) energies
- Produce protons with energies ~10 GeV-10 TeV and electrons with energies of ~0.01-10 GeV, how would we observe these particles?
- Larmor radiation ❌
- Reach us directly

Galactic Cosmic Ray Signal Below the Schwinger Limit

- Absorption length fixes average energy per particle, these are Cosmic Ray (CR) energies
- Produce protons with energies ~10 GeV-10 TeV and electrons with energies of ~0.01-10 GeV, how would we observe these particles?
- Larmor radiation ❌
- Reach us directly ❌
- Secondary signals
  - Bremsstrahlung, ionization, synchrotron radiation, and inverse Compton scattering for electrons and inelastic collisions for protons

Galactic Cosmic Ray Signal Below the Schwinger Limit

- Absorption length fixes average energy per particle, these are Cosmic Ray (CR) energies
- Produce protons with energies ~10 GeV-10 TeV and electrons with energies of ~0.01-10 GeV, how would we observe these particles?
- Larmor radiation ✖
- Reach us directly ✖
- Secondary signals ✖
    - Bremsstrahlung, ionization, synchrotron radiation, and inverse Compton scattering for electrons and inelastic collisions for protons
- Difficult to constrain ϵ in this regime

Conclusion

- Constrained broad class of "hairy" BH models using a generic and model-independent EM signal that is fully characterized by the BH mass (M) and the proportion of that mass that is lost to EM radiation (ϵ)
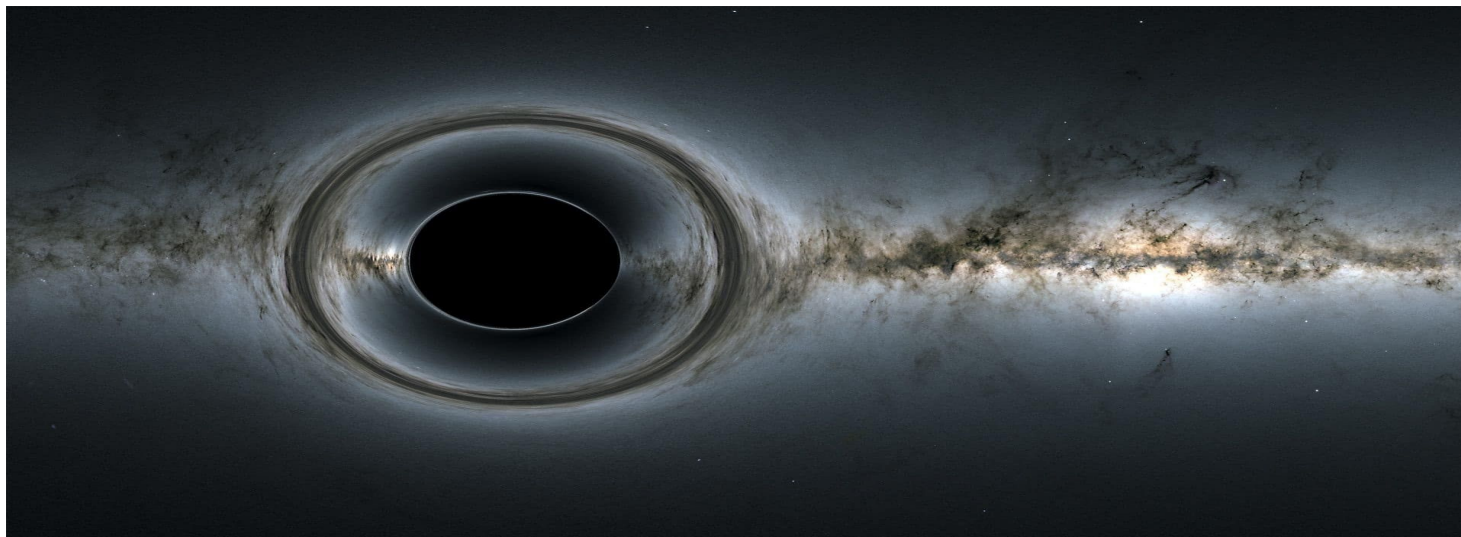
Conclusion

- Constrained broad class of "hairy" BH models using a generic and model-independent EM signal that is fully characterized by the BH mass (M) and the proportion of that mass that is lost to EM radiation (ϵ)
- Above the Schwinger limit, GRB hasn't been confidently observed from a BH-BH merger at various masses
  - $\epsilon < 10^{-5}$ for 10, 30, 40 $M_\odot$ BH and $\epsilon < 10^{-4}$ for 20, 50 $M_\odot$ BH

Conclusion

- Constrained broad class of "hairy" BH models using a generic and model-independent EM signal that is fully characterized by the BH mass (M) and the proportion of that mass that is lost to EM radiation (ϵ)
- Above the Schwinger limit, GRB hasn't been confidently observed from a BH-BH merger at various masses
  - $\epsilon < 10^{-5}$ for 10, 30, 40 M$_\odot$ BH and $\epsilon < 10^{-4}$ for 20, 50 M$_\odot$ BH
- Below the Schwinger limit, this effect produces CRs that would be difficult to observe directly.
  - BH-BH merger on strong magnetic field background could produce X-rays through synchrotron radiation
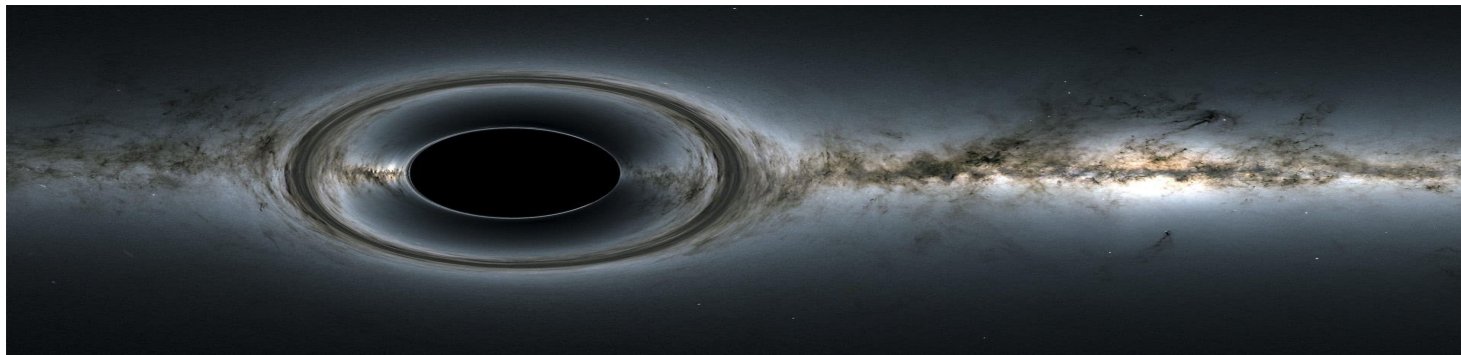
Conclusion

- Constrained broad class of "hairy" BH models using a generic and model-independent EM signal that is fully characterized by the BH mass (M) and the proportion of that mass that is lost to EM radiation (ϵ)
- Above the Schwinger limit, GRB hasn't been confidently observed from a BH-BH merger at various masses
  - $\epsilon < 10^{-5}$ for 10, 30, 40 M⊙ BH and $\epsilon < 10^{-4}$ for 20, 50 M⊙ BH
- Below the Schwinger limit, this effect produces CRs that would be difficult to observe directly.
  - BH-BH merger on strong magnetic field background could produce X-rays through synchrotron radiation
- Motivates observing BH-BH mergers with gamma-ray and X-ray telescopes

REFERENCES

Aasi, J., Abadie, J., Abbott, B. P., et al. 2015, Classical and Quantum Gravity, 32, 115012. https://ui.adsabs.harvard.edu/abs/2015CQGra..32k5012A

Abbott, B. P., Abbott, R., Abbott, T. D., et al. 2016, ApJL, 826, L13. https://ui.adsabs.harvard.edu/abs/2016ApJ...826L..13A

Acernese, F., Agathos, M., Agatsuma, K., et al. 2015, Classical and Quantum Gravity, 32, 024001. https://ui.adsabs.harvard.edu/abs/2015CQGra..32b4001A

Ares de Parga, G., & Mares, R. 1999, Journal of Mathematical Physics, 40, 4807. https://ui.adsabs.harvard.edu/abs/1999JMP....40.4807A

Aso, Y., Michimura, Y., Somiya, K., et al. 2013, PhRvD, 88, 043007. https://ui.adsabs.harvard.edu/abs/2013PhRvD..88d3007A

Broderick, A. E., Johannsen, T., Loeb, A., & Psaltis, D. 2014, ApJ, 784, 7. https://ui.adsabs.harvard.edu/abs/2014ApJ...784....7B

Canto, J. 1977, A&A, 61, 641. https://ui.adsabs.harvard.edu/abs/1977A&A....61..641C

Connaughton, V., Burns, E., Goldstein, A., et al. 2016, ApJL, 826, L6

Dai, L., McKinney, J. C., & Miller, M. C. 2017, MNRAS, 470, L92. https://ui.adsabs.harvard.edu/abs/2017MNRAS.470L..92D

Dermer, C. D. 2013, Saas-Fee Advanced Course, 40, 225. https://ui.adsabs.harvard.edu/abs/2013SAAS...40..225D

Kaplan, D. E., & Rajendran, S. 2019, PhRvD, 99, 044033. https://ui.adsabs.harvard.edu/abs/2019PhRvD..99d4033K

Kimura, S. S., Takahashi, S. Z., & Toma, K. 2017, MNRAS, 465, 4406. https://ui.adsabs.harvard.edu/abs/2017MNRAS.465.4406K

Kumar, P., & Zhang, B. 2015, PhR, 561, 1. https://ui.adsabs.harvard.edu/abs/2015PhR...561....1K

Landau, L. D., & Lifshitz, E. M. 1975, The classical theory of fields. https://ui.adsabs.harvard.edu/abs/1975ctf..book.....L

Loeb, A. 2016, ApJL, 819, L21. https://ui.adsabs.harvard.edu/abs/2016ApJ...819L..21L

Penrose, R. 1965, Phys. Rev. Lett., 14, 57. https://link.aps.org/doi/10.1103/PhysRevLett.14.57

Perna, R., Lazzati, D., & Giacomazzo, B. 2016, ApJL, 821, L18. https://ui.adsabs.harvard.edu/abs/2016ApJ...821L..18P

Piran, T. 1999, PhR, 314, 575. https://ui.adsabs.harvard.edu/abs/1999PhR...314..575P

Psaltis, D., Wex, N., & Kramer, M. 2016, ApJ, 818, 121. https://ui.adsabs.harvard.edu/abs/2016ApJ...818..121P

Qi, H., O'Shaughnessy, R., & Brady, P. 2021, PhRvD, 103, 084006. https://ui.adsabs.harvard.edu/abs/2021PhRvD.103h4006Q

Raju, S. 2022, PhR, 943, 1. https://ui.adsabs.harvard.edu/abs/2022PhR...943....1R

Fedrow, J. M., Ott, C. D., Sperhake, U., et al. 2017, PhRvL, 119, 171103. https://ui.adsabs.harvard.edu/abs/2017PhRvL.119q1103F

Goodman, J. 1986, ApJL, 308, L47. https://ui.adsabs.harvard.edu/abs/1986ApJ...308L..47G

Hawking, S. W. 1975, Communications in Mathematical Physics, 43, 199. https://ui.adsabs.harvard.edu/abs/1975CMaPh..43..199H

Hawking, S. W. 1976, Phys. Rev. D, 14, 2460. https://link.aps.org/doi/10.1103/PhysRevD.14.2460

Heisenberg, W., & Euler, H. 1936, Z. Phys., 98, 714. https://arxiv.org/abs/physics/0605038

Isi, M., Giesler, M., Farr, W. M., Scheel, M. A., & Teukolsky, S. A. 2019, PhRvL, 123, 111102. https://ui.adsabs.harvard.edu/abs/2019PhRvL.123k1102I

Longair, M. S. 1992, High energy astrophysics. Vol.1: Particles, photons and their detection

—. 1994, High energy astrophysics. Vol.2: Stars, the galaxy and the interstellar medium, Vol. 2

Lyutikov, M. 2016, arXiv e-prints, arXiv:1602.07352. https://ui.adsabs.harvard.edu/abs/2016arXiv160207352L

Mandel, I., & Mink, S. 2015, Monthly Notices of the Royal Astronomical Society, 458, doi:10.1093/mnras/stw379. https://arxiv.org/abs/1601.00007

Özel, F., Psaltis, D., Narayan, R., & McClintock, J. E. 2010, ApJ, 725, 1918. https://ui.adsabs.harvard.edu/abs/2010ApJ...725.1918O

Parikh, M. K., & Wilczek, F. 2000, PhRvL, 85, 5042

Reynolds, R. J. 1990, The Low Density Ionized Component of the Interstellar Medium and Free-Free Absorption at High Galactic Latitudes, ed. N. E. Kassim & K. W. Weiler, Vol. 362, 121

Reynolds, R. J. 1992, AIP Conference Proceedings, 278, 156. https://aip.scitation.org/doi/abs/10.1063/1.44005

Sadeghian, L., & Will, C. M. 2011, Classical and Quantum Gravity, 28, 225029. https://ui.adsabs.harvard.edu/abs/2011CQGra..28v5029S

Schwinger, J. 1951, Phys. Rev., 82, 664. https://link.aps.org/doi/10.1103/PhysRev.82.664

Sobrinho, J., & Azevedo Freitas, S. 2021, doi:10.13140/RG.2.2.11329.07526. https://www.researchgate.net/publication/353573336_A_list_of_48_Binary_Black_Hole_mergers?enrichId=rgreq-95109f8c6a478a2c18427877587362e7-XXX&enrichSource=Y292ZXJQYWdlOzM1MzU3MzMzNjtBUzoxMDUxMjI3MTk0NDA0ODC2QDE2Mjc2NDM1MDI4NDA=&el=1_x_3&_esc=publicationCoverPdf

The Fermi GBM Collaboration. 2020, Overview of the Fermi GBM, NASA. https://fermi.gsfc.nasa.gov/ssc/data/analysis/documentation/Cicerone/Cicerone_Introduction/GBM_overview.html

Wang, D. 2022a, arXiv e-prints, arXiv:2205.08026. https://ui.adsabs.harvard.edu/abs/2022arXiv220508026W

Wang, K. 2022b, European Physical Journal C, 82, 125. https://ui.adsabs.harvard.edu/abs/2022EPJC...82..125W

Woosley, S. E. 2016, ApJL, 824, L10. https://ui.adsabs.harvard.edu/abs/2016ApJ...824L..10W

Zhang, B. 2016, ApJL, 827, L31. https://ui.adsabs.harvard.edu/abs/2016ApJ...827L..31Z

Preliminaries Backup

Hawking radiation (Parikh & Wilczek 2000). Thus, the characteristic frequency of the emitted photons is the same as that of Hawking radiation. If the Schwarzschild radius of a BH is given by

$$r_s = M r_{s,\odot} \text{ MeV}^{-1} \tag{1}$$

where M is the BH mass in solar units ($M = \frac{M_{BH}}{M_\odot}$ where $M_\odot \sim 1.989 \times 10^{33}$ g $\sim 10^{60}$ MeV) and $r_{s,\odot} = \frac{2GM_\odot}{c^2} \sim 3 \times 10^5$ cm $\sim 10^{16}$ MeV^{-1} is the Schwarzchild radius of the Sun, then the characteristic frequency of the radiation emitted by the BH is

$$f = \frac{1}{2r_s} = \frac{1}{2Mr_{s,\odot}} \sim \frac{3 \times 10^{-17}}{M} \text{ MeV} \tag{2}$$

and wavelength is

$$\lambda = \frac{1}{f} = 2Mr_{s,\odot} \sim (3 \times 10^{16})M \text{ MeV}^{-1} \tag{3}$$

Throughout this paper, we work in natural units where $\hbar = c = k_B = \epsilon_0 = 1$ unless otherwise stated.

Schwinger Limit Backup

2. THE SCHWINGER LIMIT

The Schwinger limit dictates the critical value of ϵ separating the two phenomenologically distinct cases in which radiation is emitted for a particular BH mass. This limit, derived from quantum electrodynamics, sets the field strength at which an electric field becomes nonlinear due to the spontaneous production of electron-positron pairs (Heisenberg & Euler (1936), Schwinger (1951)). Quantitatively, the Schwinger limit occurs at an electric field strength of

$$E_C = m_e^2/e = 0.86 \text{ MeV}^2 \tag{4}$$

This corresponds to a field energy density of

$$u_C = E^2 = 0.74 \text{ MeV}^4 \tag{5}$$

This field energy density can be related to ϵ as follows. Assume the radiation from the BH is spread over a volume one wavelength (λ) in thickness outside of the BH. Then, the energy density of the BH radiation is

$$u = \frac{\epsilon M_{BH}}{\frac{4}{3}\pi((r_s + \lambda)^3 - r_s^3)} = \frac{3\epsilon M_\odot}{104\pi r_{s,\odot}^3 M^2} \sim (3 \times 10^9)\frac{\epsilon}{M^2} \text{ MeV}^4 \tag{6}$$

Setting $u = u_C$ and solving for the critical value of ϵ gives

$$\epsilon_C = \frac{104\pi m_e^4 r_{s,\odot}^3}{3e^2 M_\odot} M^2 \sim 2.4 \times 10^{-10} M^2 \tag{7}$$

Thus, $\epsilon_C \sim 10^{-10}$, 10^{-8}, 10^{-7} for a 1, 10, and 30 $M_\odot$ BH respectively. For $\epsilon > \epsilon_C$, pair-production dominates and results in a GRB as discussed in Sec. 3. For $\epsilon < \epsilon_C$, the EM field accelerates ambient charged particles, creating CR electrons and protons as discussed in Sec. 4.

Gamma-ray Emission Above the Schwinger Limit
Backup 1

When the EM radiation is first emitted by the BH, the lab and fluid frames coincide. Thus, the initial temperature of the fireball in both S and S' is given by

$$T_0 = \left(\frac{E}{V_0 g_0 a} \right)^{1/4} \tag{8}$$

where $a = \pi^2/15$, E is the energy dumped into a region of volume V_0, and $g_0 = 2.75 = 11/4$ is half of the effective degrees of freedom for a plasma consisting of photons, electrons, and positrons in thermal equilibrium. Again assuming that the radiation from the BH is spread over a volume one wavelength in thickness outside of the BH, the initial temperature is

$$T_0 = \left(\frac{\epsilon M_{BH}}{\frac{4}{3}\pi((r_s + \lambda)^3 - r_s^3)\frac{11}{4}a} \right)^{1/4} = \left(\frac{45 \epsilon M_\odot}{286 \pi^3 M^2 r_{s,\odot}^3} \right)^{1/4} \sim 200 \left(\frac{\epsilon}{M^2} \right)^{1/4} \text{ MeV} \tag{9}$$

Since the ISM is very diffuse, we assume that the fireball expands adiabatically into the vacuum. In the case of adiabatic expansion, no work is done by the fluid and the temperature of the fireball remains constant in the lab frame so long as the fireball is opaque due to Thompson scattering. That is,

$$T(r) = T_0 \tag{10}$$

However, in the comoving frame of the fluid, the fireball cools as it expands.

$$T'(r) = \frac{T_0}{\gamma(r)} \tag{11}$$

where the Lorentz factor of the fireball varies with distance from the BH as $\gamma(r) \propto r$.

Since the number density of electron-positron pairs in the comoving frame of the fluid depends on T' as $n' \propto T'^{3/2} e^{-m_e/T'}$, the number density of pairs decreases as the fireball cools. Eventually,

the process of pair creation and annihilation freezes out when the time for a positron to annihilate with an electron is of the same order as the dynamical time. This occurs at a comoving temperature of $T' \sim 20$ keV. At this temperature, the amount of the initial energy from the BH contained in the remaining electron-positron pairs is negligible. Rather, $O(1)$ of the initial ϵM_{BH} is contained in photons that had been trapped in the fluid by Thompson scattering. When pair production freezes out, the Thompson opacity decreases dramatically and these photons escape.

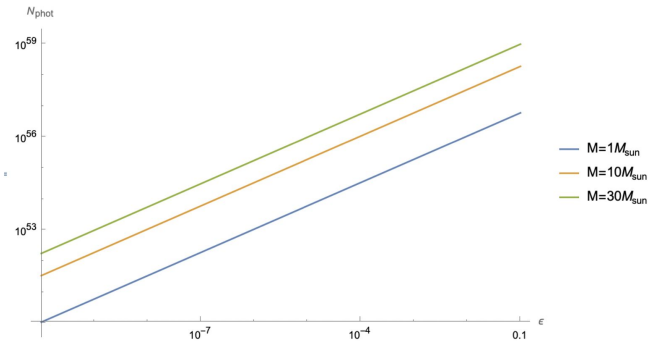# Gamma-ray Emission Above the Schwinger Limit Backup 2

Figure 2. This plot shows the number of photons emitted for a 1, 10, and 30 $M_\odot$ BH at various ϵ.

When the photons are able to free stream from the fireball, an observer on Earth will see a black body spectrum at temperature T_0 radiating from the BH. The black body spectrum in photon number as a function of photon frequency and the fireball temperature is given by

$$B_f(T_0) = \frac{2f^2}{e^{2\pi f/T_0} - 1} \text{ MeV}^2 \text{ s}^{-1} \text{ Hz}^{-1} \text{ ster}^{-1} \tag{12}$$

Taking the derivative with respect to the photon frequency, f, gives an equation for the peak in the spectrum. This peak occurs when

$$e^{2\pi f/T_0}(\pi f - T_0) + T_0 = 0 \tag{13}$$

which has the solution $f_{peak} \sim \frac{1.6 T_0}{2\pi}$. Thus, the peak photon energy is

$$E_{peak} = 1.6 T_0 = 1.6 \left(\frac{45 \epsilon M_\odot}{286 \pi^3 M^2 r_{s,\odot}^3} \right)^{1/4} \sim 320 \left(\frac{\epsilon}{M^2} \right)^{1/4} \text{ MeV} \tag{14}$$

These peak energies are plotted in Fig. 1 as a function of BH mass and ϵ. These are the most likely photons to be emitted from the fireball, and all peak energies are gamma rays (energy > 1 MeV).

Since order one of the energy from the fireball is converted into photons at the peak energy, the number of photons emitted is

$$N_\gamma = \frac{\epsilon M_{BH}}{E_{peak}} = \frac{1}{1.6} \left(\frac{286}{45} \pi^3 \right)^{1/4} r_{s,\odot}^{3/4} M_\odot^{3/4} \epsilon^{3/4} M^{3/2} \sim (3.4 \times 10^{57}) \epsilon^{3/4} M^{3/2} \tag{15}$$

The number of photons emitted for a 1, 10, and 30 $M_\odot$ BH at various ϵ is plotted in Fig. 2.

Gamma-ray Emission Above the Schwinger Limit
Backup 3

Over the full range of photon energies shown in Fig. 1, the most sensitive telescope is the Fermi Gamma-ray Space Telescope. The two instruments onboard Fermi are the Large Area Telescope (LAT) and the Gamma-ray Burst Monitor (GBM). The LAT observes photon energies in the range 20 MeV -300 GeV with a sensitivity of 10^{-4} erg cm^{-2} (Dermer 2013). The GBM observes photon energies in the range 8 keV -40 MeV with a sensitivity of 0.5 ph cm^{-2} s^{-1} (The Fermi GBM Collaboration 2020). At the gamma-ray energies emitted by 1-30 $M_\odot$ BHs over a timescale of $\lesssim 1$ second, Fermi's sensitivity limits requires a flux of ~ 1 ph cm^{-2}. This minimum flux can be used to calculate the maximum distance, d, to which EM emission by a BH above the Schwinger limit would be observable.
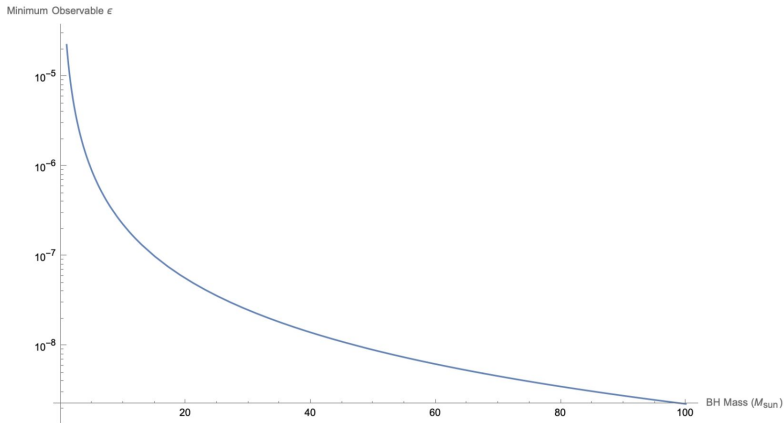

Figure 4. This plot shows the minimum ϵ for which Fermi could observe such an event to > 100 Mpc as a function of BH mass. For the 1, 10, and 30 $M_\odot$ BHs respectively, any $\epsilon \geq 10^{-4}$, 10^{-6}, and 10^{-7} would be observable to > 100 Mpc.

$$d = \sqrt{\frac{N_\gamma}{4\pi}} = \sqrt{\frac{1}{6.4\pi}\left(\frac{286}{45}\pi^3\right)^{1/4} r_{s,\odot}^{3/4} M_\odot^{3/4} \epsilon^{3/4} M^{3/2}} \sim (1.7 \times 10^{28})\epsilon^{3/8}M^{3/4} \text{ cm} \qquad (17)$$

These distances are plotted in Fig. 3.

As stated in Sec. 1, for a BBH merger trigger this signal must be observable to at least $d > 100$ Mpc $\sim 3 \times 10^{26}$ cm. Thus, we can solve for the minimum ϵ for which Fermi could observe such an event extragalactically.

$$\epsilon_{min} = \left(\frac{3 \times 10^{26}}{\sqrt{\frac{1}{6.4\pi}\left(\frac{286}{45}\pi^3\right)^{1/4} r_{s,\odot}^{3/4} M_\odot^{3/4}}}\right)^{8/3} M^{-2} \sim \frac{2 \times 10^{-5}}{M^2} \qquad (18)$$

These minimum values of ϵ are plotted in Fig. 4 as a function of BH mass. For the 1, 10, and 30 $M_\odot$ BHs respectively, any $\epsilon \geq 10^{-4}$, 10^{-6}, and 10^{-7} would be observable to > 100 Mpc.

Gamma-ray Emission Above the Schwinger Limit Backup 4

The Gravitational-wave Transient Catalog (GWTC) lists events detected by the Advanced Laser Interferometer Gravitational-Wave Observatory (LIGO, Aasi et al. (2015)), Virgo (Acernese et al. 2015), and the Kamioka Gravitational Wave Detector (KAGRA, Aso et al. (2013)). Most BBH merger candidates listed in the GWTC are posted on NASA's General Coordinates Network (GCN). The GCN is a platform for astronomers to collaborate and alert each other to objects that may benefit from multi-messenger observations, especially transient events. This network facilitates both concurrent and follow-up EM observations of GW triggers, including observations by the Fermi GBM of the LIGO/Virgo 90% confidence localization region (LR) for each posted event. The Fermi GBM has an 8 steradian field-of-view (The Fermi GBM Collaboration 2020), which is large enough to cover the full LR if the telescope is well-aligned at the time of the trigger. We cross-referenced all BBH mergers in the GWTC with Fermi GBM observations from the GCN. For BH masses ranging from 10 to 50 $M_\odot$ in intervals of 10 $M_\odot$, we identified the nearest BBH merger for which Fermi observed at least 90% of the LR and recorded no GRB event. The GW events constraining each mass interval are listed in Tab. 1. These non-detections were used to constrain ϵ for each BH mass. To do this, we assumed the the furthest distance (luminosity distance + error bar) measured by LIGO/Virgo and calculated the minimum value of ϵ needed such that the event would be observable with the Fermi GBM for the observed BH mass. All constrained values of ϵ were above the Schwinger limit for the given BH mass and all resulted in $\sim$ MeV photons which are in the energy range observable by the GBM. These constraints are listed in Tab. 2, assuming all BHs are "hairy" BHs capable of producing this signal. The current upper bounds on ϵ are $\epsilon < 10-5$ for 10, 30, 40 $M_\odot$ BHs and $\epsilon < 10-4$ for 20, 50 $M_\odot$ BHs since no high energy EM signal was observed from these BBH mergers. These constraints will improve as Fermi continues to monitor the sky.

Gamma-ray Emission Above the Schwinger Limit Backup 5

There has been one observation of a GRB and BBH merger occurring concurrently. An offline search of Fermi-GBM data following the detection of GW150914 (Abbott et al. 2016) revealed a 1 second short GRB occurring 0.4 seconds after the LIGO trigger with a localization consistent with that of the GW signal (Connaughton et al. 2016). The LIGO localization map overlaid with the Fermi-GBM observation region is shown in Fig. 1 in Connaughton et al. (2016) and has also

been reproduced below in Fig. 5. However, the GRB transient was near the detection threshold for the GBM (2.9σ detection), was not detected by any other instrument, and the localization was poorly constrained (Connaughton et al. 2016). Thus, the GRB cannot be confidently associated with GW150914. Assuming that the GRB did indeed originate from the BBH merger, we can identify the range of ϵ that is consistent with the measured properties of the merger and GRB. From the GWTC, the constituent BH masses range from $\sim$30-40 $M_\odot$ and the range of luminosity distances is 270-590 Mpc. For these masses and distances, the minimum value of ϵ such that the event would be observable with the Fermi-GBM ranges from $\epsilon_{min} \sim 10^{-7} - 10^{-6}$ resulting in peak photon energies of $\sim 1 - 3$ MeV. This range of peak photon energies is consistent with the properties of the observed GRB, which peaked near an MeV (Connaughton et al. 2016). Since this event was barely above Fermi-GBM's SNR, we anticipate $\epsilon \sim \epsilon_{min}$. Thus, the observed GRB is consistent with a GRB produced via rapid EM emission by a 30-40 $M_\odot$ BH for $\epsilon \sim 10^{-7} - 10^{-6}$.

Galactic Cosmic Ray Signal Below the Schwinger Limit Backup 1

First, consider the acceleration of a single charged particle due to a strong EM pulse that is one wavelength in duration. In the (+ - - -) metric, the relativistic Lorentz force law is

$$\frac{du^\alpha}{d\tau} = \frac{e}{m} F^{\alpha\beta} u_\beta \tag{20}$$

where e is the elementary charge, m is the proton or electron mass, u^α is the particle's 4-velocity, and τ is the proper time in the instantaneous rest frame of the particle. The characteristic BH wavelength is long relative to the amplitude of the wave, so we assume that the field magnitude is constant. Additionally, this long wavelength causes the system to behave like a linear accelerator and thus the charged particle radiates a negligible amount. This can be verified explicitly by solving the Landau-Lifshitz equation for radiation reaction (Landau & Lifshitz 1975) for a constant crossed field (Ares de Parga & Mares 1999). We also neglect any special relativistic effects that transform the field in the instantaneous rest frame of the particle. As will be shown later, even for an initial field strength right at the Schwinger limit, the absorption length for the EM field is long enough that the average charged particle experiences a sufficiently weak field for these effects to be neglected. Choose a coordinate system such that the electric field is directed along the x-axis and the magnetic field along the y-axis, then the Faraday tensor is

$$F^{\alpha\beta} = \begin{pmatrix} 0 & -E & 0 & 0 \\ E & 0 & 0 & 0 \\ 0 & 0 & 0 & E \\ 0 & 0 & -E & 0 \end{pmatrix} \tag{21}$$

Since $\frac{e}{m}F^{\alpha\beta}$ is constant, the Lorentz force equation has a simple exponential solution.

$$u^\alpha(\tau) = \exp\left(\frac{e}{m}\tau F^\alpha_\beta\right) u^\beta(0) \tag{22}$$

The particles accelerate from the thermal speed of the plasma $(v \sim 0)$, fixing the initial 4-velocity as

$$u^\beta(0) = \begin{pmatrix} 1 \\ 0 \\ 0 \\ 0 \end{pmatrix} \tag{23}$$

Computing $u^\alpha(\tau)$ for the given Faraday tensor yields

$$u^\alpha(\tau) = \begin{pmatrix} 1 + \frac{e^2 E^2 \tau^2}{2m^2} \\ \frac{eE\tau}{m} \\ 0 \\ \frac{e^2 E^2 \tau^2}{2m^2} \end{pmatrix} \tag{24}$$

which can be used to extract the Lorentz factor, γ, and the components of the 3-velocity in the lab frame, $\mathbf{v}$.

$$\gamma(\tau) = 1 + \frac{e^2 E^2 \tau^2}{2m^2} \tag{25}$$

$$v_x(\tau) = \frac{2eEm\tau}{2m^2 + e^2 E^2 \tau^2} \tag{26}$$

$$v_y(\tau) = 0 \tag{27}$$

$$v_z(\tau) = 1 - \frac{2m^2}{2m^2 + e^2 E^2 \tau^2} \tag{28}$$

These are plotted in Figs. 5, 6 as the a function of the particle's proper time spent in the EM field for field amplitudes of 0.86 and 10^{-10} MeV^2. Initially, the particle is accelerated in the $\pm$x-direction. But, as τ increases, $|v_x| \to 0$ and $v_z \to 1$, with v_z approaching 1 more rapidly for larger field amplitudes.

Galactic Cosmic Ray Signal Below the Schwinger Limit Backup 2

The final kinetic energy of the particle depends on the time at which the particle exits the field in its instantaneous rest frame, τ_f. By definition, $\gamma(\tau) = \frac{dt}{d\tau}$. Thus,

$$\int_0^{\tau_f} \gamma(\tau)d\tau = \tau_f + \frac{e^2 E^2 \tau_f^3}{6m^2} = \int_0^{t_f} dt = \frac{1}{f} \tag{29}$$

since in the lab frame the particle is in the field for $t_f = \frac{1}{f}$ where f is the frequency of the BH radiation. As long as the magnitude of the electric field is not too small, we can neglect the term that is linear in τ_f and find

$$\tau_f = \left(\frac{6m^2}{e^2 E^2 f} \right)^{1/3} = \left(\frac{12m^2 r_{s,\odot}}{e^2 E^2} M \right)^{1/3} \sim (1 \times 10^8) \left(\frac{M}{E^2} \right)^{1/3} \text{ MeV}^{-1} \tag{30}$$

Where here, and in all following numerical expressions, we set $m = m_p$. As will be discussed later, average field magnitudes are sufficiently large for the range of values of ϵ that are of interest and so this approximation holds.

Galactic Cosmic Ray Signal Below the Schwinger Limit Backup 3

Consider the total energy, E_{in}, of a shell one wavelength in thickness j wavelengths from the event horizon of the BH. Assuming j is large, the initial energy density is

$$u = \frac{E_{in}}{\frac{4}{3}\pi[(r_s + j\lambda)^3 - (r_s + (j-1)\lambda)^3]} \sim \frac{E_{in}}{4\pi\lambda^3 j^2} = \frac{E_{in}}{32\pi(Mr_{s,\odot})^3 j^2} \sim (3 \times 10^{-51})\frac{E_{in}}{M^3 j^2} \text{ MeV}^4 \quad (31)$$

Then the magnitude of the electric field is

$$E = \sqrt{u} \sim \sqrt{\frac{E_{in}}{32\pi(Mr_{s,\odot})^3 j^2}} \sim (5 \times 10^{-26})\sqrt{\frac{E_{in}}{M^3 j^2}} \text{ MeV}^2 \quad (32)$$

The kinetic energy of each proton after interacting with the EM wave is

$$K \sim \gamma(\tau_f)m \quad (33)$$
$$\sim \frac{e^2 E^2 \tau_f^2}{2m} \quad (34)$$
$$= \frac{1}{2}\left(\frac{9me^2 E_{in}}{2\pi r_{s,\odot} j^2 M}\right)^{1/3} \quad (35)$$
$$\sim (1 \times 10^{-5})\left(\frac{E_{in}}{j^2 M}\right)^{1/3} \text{ MeV} \quad (36)$$

This gives the kinetic energy of one proton in the jth shell. We assume a homogeneously distributed number density of charged particles with $n = n_p = n_e \sim 1 \text{ cm}^{-3} \sim 10^{-32} \text{ MeV}^3$, consistent with the Milky Way ISM (Canto 1977; Reynolds 1992). Thus, the total number of protons in the jth shell is

$$N = \frac{4}{3}\pi n[(r_s + j\lambda)^3 - (r_s + (j-1)\lambda)^3] \sim 4\pi n\lambda^3 j^2 = 32\pi n(Mr_{s\odot})^3 j^2 \sim (3 \times 10^{18}) j^2 M^3 \quad (37)$$

So the total kinetic energy absorbed in the jth shell is

$$K_{tot} \sim 8n(36\pi^2 me^2 r_{s,\odot}^8 M^8 j^4 E_{in})^{1/3} \sim (3 \times 10^{13})(M^8 j^4 E_{in})^{1/3} \text{ MeV} \quad (38)$$

This gives a differential equation for the energy absorbed by the field

$$\frac{dE_{in}}{dj} = -K_{tot} \quad (39)$$

subject to the initial condition $E_{in}(0) = \epsilon M_{BH}$. This equation can be integrated to yield

$$E_{in}(j) = \left((\epsilon M_{BH})^{2/3} - \frac{16}{7}n(36\pi^2 me^2 r_{s,\odot}^8 M^8)^{1/3} j^{7/3}\right)^{3/2} \quad (40)$$

An example plot of the fractional energy remaining in the field as a function of distance from the BH is shown in Fig. 7.

Galactic Cosmic Ray Signal Below the Schwinger Limit Backup 4

The absorption length, j_{abs}, gives the number of protons accelerated by the field

$$N_{abs} = \frac{4}{3}\pi n (j_{abs}\lambda)^3 \sim (7\times 10^{52})\epsilon^{6/7}M^{3/7} \tag{42}$$

Thus, $E_{in}(j) = 0$ when $(\epsilon M_{BH})^{2/3} = \frac{16}{7}n(36\pi^2 m e^2 r_{s,\odot}^8 M^8)^{1/3}j^{7/3}$. Solving for the j at which this occurs gives the absorption length

Note that the number of electrons accelerated by the field is also N_{abs}. This gives the average kinetic energy, speed, and Lorentz factor of each proton.

$$j_{abs} = \left(\frac{7(\epsilon M M_\odot)^{2/3}}{16n(36\pi^2 m e^2 r_{s,\odot}^8 M^8)^{1/3}}\right)^{3/7} \sim (4\times 10^{11})\frac{\epsilon^{2/7}}{M^{6/7}} \tag{41}$$

$$KE_{avg} = \frac{\epsilon M_{BH}}{N_{abs}} \sim (2\times 10^7)\epsilon^{1/7}M^{4/7} \text{ MeV} \tag{43}$$

$$v_{avg} = \sqrt{1-(m/KE_{avg})^2} \sim \sqrt{1-\frac{4\times 10^{-9}}{\epsilon^{2/7}M^{8/7}}} \tag{44}$$

$$\gamma_{avg} = \frac{1}{\sqrt{1-v_{avg}^2}} \sim (2\times 10^4)\epsilon^{2/14}M^{8/14} \tag{45}$$

We also obtain the average field experienced by the protons from the field strength for which $\gamma(\tau_f, E_{avg}) = \gamma_{avg}$, such that

$$E_{avg} = \sqrt{\frac{2m^2}{e^2\tau_f^2}(\gamma_{avg}-1)} \tag{46}$$

Right at the Schwinger limit, the average field strength is $\sim 10^{-9}$ MeV^2 for a 1-30 $M_\odot$ BH. For $\epsilon = 10^{-20}$, this average field strength decreases to $\sim 10^{-12}$ MeV^2. Thus, for the range of ϵ considered here, the average field strength is weak enough to allow us to neglect the special relativistic effects which transform the field but strong enough that the earlier approximation for τ_f holds.

Galactic Cosmic Ray Signal Below the Schwinger Limit Backup 5

We perform this calculation for values of ϵ ranging from $\epsilon = 10^{-20}$ to the Schwinger limit ($\epsilon = 10^{-10}$ for a 1 $M_\odot$ BH, 10^{-8} for a 10 $M_\odot$ BH, and 10^{-7} for a 30 $M_\odot$ BH). The resulting average proton kinetic energies as a function of ϵ are plotted in Fig. 9. For the 1 $M_\odot$ BH, the average kinetic energy per proton ranges from 22 GeV for $\epsilon = 10^{-20}$ to 582 GeV for $\epsilon = 10^{-10}$. For the 10 $M_\odot$ BH, the average kinetic energy per proton ranges from 81 GeV for $\epsilon = 10^{-20}$ to 4190 GeV for $\epsilon = 10^{-10}$. For the 30 $M_\odot$ BH, the average proton kinetic energy per proton ranges from 152 GeV for $\epsilon = 10^{-20}$ to 11 TeV for $\epsilon = 10^{-10}$.

The average proton kinetic energies can be used to calculate the corresponding average electron kinetic energies, since $\gamma_p = \gamma_e$. For the 1 $M_\odot$ BH, the average kinetic energy per electron ranges from 0.01 GeV for $\epsilon = 10^{-20}$ to 0.3 GeV for $\epsilon = 10^{-10}$. For the 10 $M_\odot$ BH, the average kinetic energy

19

per electron ranges from 0.04 GeV for $\epsilon = 10^{-20}$ to 2.3 GeV for $\epsilon = 10^{-10}$. For the 30 $M_\odot$ BH, the average kinetic energy per electron ranges from 0.08 GeV for $\epsilon = 10^{-20}$ to 5.9 GeV for $\epsilon = 10^{-10}$.

Now we consider the ways in which a signal from BH emission below the Schwinger limit might (or might not) be observed. Since the protons and electrons are rapidly accelerated to $v \sim 1$, they emit negligible Larmor radiation. Thus, there is no signal during the initial acceleration phase of the charged particles. Additionally, there can be no direct extra-galactic signal from these particles. Because ambient magnetic fields constrain CRs with energies $\lesssim 10^6$ GeV to their host galaxies, these protons and electrons cannot escape their host galaxy to reach an Earth observer.

The cloud of ultra-relativistic protons and electrons also cannot be easily detected directly or indirectly from a source in the Milky Way. The Milky Way has a background magnetic field of strength $B \sim 3 \times 10^{-10}$ T (Longair 1994). As these particles travel, inhomogeneities in this background field affect the charged particle's trajectory and cause it to diffuse into the galactic CR background. The maximum length of this diffusion scale is the Larmor radius of the particle in the magnetic field, which, in SI units, is

$$R = \frac{\gamma m v}{q B} \tag{47}$$

Here $v \sim c$ and the maximum possible average γ is $\sim 10^4$ (for a 30 $M_\odot$ BH at the Schwinger limit). So, the maximum possible Larmor radius is $R \sim 0.01$ ly for a proton and $\sim 10^{-5}$ ly for an electron. Since the Milky Way is $\sim 10^5$ ly across, this distance is negligible on galactic scales and these ultra-relativistic particles diffuse into the galactic CR background.

Similarly, the timescales for the production of secondary signals from the ultra-relativistic charged particles are too long to observe. Ultra-relativistic electrons can radiate via a variety of processes such as bremsstrahlung, ionization, synchrotron radiation, and inverse Compton scattering (Longair 1992, 1994). However, the shortest timescale for a 0.01-10 GeV electron to lose order one of its energy to any of these mechanisms is $\sim 10^6$ years, and is thus too long for the radiation to be observable. Ultra-relativistic protons are too massive to radiate appreciably. Instead, they primarily lose energy by inelastically colliding with stationary nuclei in the ISM to produce pions, gamma-rays, electrons, positrons, and neutrinos (Longair 1992, 1994). The mean lifetime for a 20-10^4 GeV proton to undergo such a collision, for Milky Way ISM densities, is $\sim 10^7$ yr. As with the electrons, the proton lifetime for this process is so long that the products would not be observable.

Thus, below the Schwinger limit, it becomes difficult to place strong constraints on ϵ. In most cases, this signal would appear at best as an overabundance of diffuse CR protons and electrons. However, such an excess would be explainable by standard astrophysical objects such as a nearby quasar.